JOURNAL

OF THE AMERICAN CHEMICAL SOCIETY

VOLUME 109, NUMBER 7 APRIL 1, 1987

Hydration and Energetics for $(CH_3)_3CCl$ Ion Pairs in Aqueous Solution†

William L. Jorgensen,*‡ J. Kathleen Buckner,‡ Shawn E. Huston,§ and Peter J. Rossky§

Contribution from the Herbert C. Brown Laboratory of Chemistry, Purdue University, West Lafayette, Indiana 47907, and the Department of Chemistry, University of Texas at Austin, Austin, Texas 78712. *Received November 10, 1986*

Abstract: Free-energy profiles have been computed for the separation of *tert*-butyl cation and chloride ion in dilute aqueous solution at 25 °C and 1 atm. The theoretical approach features both extensive Monte Carlo simulations using statistical perturbation theory and integral equation calculations using extended RISM methodology. The necessary carbenium ion–water potential functions were obtained from ab initio molecular orbital calculations with the 6-31G(d) basis set, while previously reported potential functions were adopted for the other interactions. The Monte Carlo simulations predict the occurrence of a contact ion pair at a C–Cl distance of 2.9 Å and the onset of the solvent-separated ion-pair regime near 5.5 Å; however, solvent-separated ion pairs and "free" ions are not found to be energetically distinct species. There is a barrier of 2 kcal/mol between the contact and solvent-separated ion pairs. The latter is found to be 4 kcal/mol lower in free energy and ca. 2 kcal/mol below the infinitely separated ions. The extended RISM result for the free-energy profile is similar in shape, but the features have much smaller amplitude. Detailed structural characterization of the changes in hydration as a function of interionic distance has also been obtained; the insertion of a water molecule between the ions occurs between 5.0 and 5.5 Å.

The ion pair mechanism in eq 1 was developed by Winstein and co-workers to account for the kinetics and stereochemistry

$$R\text{–}X \rightleftharpoons R^+X^- \rightleftharpoons R^+//X^- \rightleftharpoons R^+ + X^- \qquad (1)$$

of solvolysis reactions.[1,2] In this scheme, R^+X^-, $R^+//X^-$, and $R^+ + X^-$ represent contact ion pairs, solvent-separated ion pairs, and the free ions which can all lead to products. Nevertheless, despite the extensive research on solvolysis and substitution reactions,[3-5] relatively little is known about the details of the associated free energy surfaces in solution. In view of this and the general interest in aqueous ionic solutions,[6,7] we set out to calculate the energy profile for the ion pair region in the hydrolysis of 2-chloro-2-methylpropane (*t*-BuCl) using new theoretical methods that can provide results of acceptable precision.

An energy profile similar to the one in Figure 1 has previously been suggested by Abraham for solvolysis of this parent tertiary halide.[8] However, about all that is well-established in water is $\Delta G^\ddagger = 19.5$ kcal/mol[9] and the transition state is structurally close to the contact ion pair with ca. 80% charge separation.[8] In another paper, Abraham provided a thermodynamic analysis that placed $t\text{-Bu}^+\text{Cl}^-$ and the fully separated ions at about the same free energy, 14.5 kcal/mol above the reactant.[10] This implies a $\Delta G^\ddagger$ of ca. 5 kcal/mol for collapse of the contact ion pair back to reactants, though the uncertainties in Abraham's analysis are at least ±5 kcal/mol. Few closely related data are available except some dynamic NMR results for collapse of trityl and tropylium chloride ion pairs.[11] In both the NMR work and Abraham's analysis, solvent-separated ion pairs are not included as distinct entities.

Some additional background information is also worth noting. In 1940, Ingold and co-workers reported their findings on salt effects for the hydrolysis of *t*-BuBr.[12] They observed the normal salt effect with increasing ionic strength of the medium; however, common ion rate depression was only found for more stable carbenium ions. Consistently, solvolysis of *t*-BuCl in aqueous methanol with added $Na^{36}Cl$ revealed only slight chloride exchange.[13] Thus, the lifetime for $t\text{-Bu}^+$ in aqueous media is short

† Dedicated to Professor Herbert C. Brown on the occasion of his 75th birthday.

‡ Purdue University.

§ University of Texas.

(1) Winstein, S.; Clippinger, E.; Fainberg, A. H.; Robinson, G. C. *J. Am. Chem. Soc.* **1954**, *76*, 2597.
(2) Raber, D. J.; Harris, J. M.; Schleyer, P. v. R. In *Ions and Ion Pairs in Organic Reactions*; Szwarc, M., Ed.; Wiley: New York, 1974; Vol. 2, p 247.
(3) Streitwieser, A. *Chem. Rev.* **1956**, *56*, 571.
(4) Brown, H. C. *The Nonclassical Ion Problem*; Plenum: New York, NY, 1977.
(5) Olah, G. A.; Schleyer, P. v. R., Eds. *Carbonium Ions*; Wiley: New York, NY, 1968–1973; Vol. I–IV.
(6) Wolynes, P. G. *Annu. Rev. Phys. Chem.* **1980**, *31*, 345. Friedman, H. *Ibid.* **1981**, *32*, 179.
(7) Pettitt, B. M.; Rossky, P. J. *J. Chem. Phys.* **1986**, *84*, 5836.
(8) Abraham, M. H. *Prog. Phys. Org. Chem.* **1974**, *11*, 1.
(9) (a) Winstein, S.; Fainberg, A. H. *J. Am. Chem. Soc.* **1957**, *79*, 5937. (b) Robertson, R. E.; Heppolette, R. L.; Scott, J. M. W. *Can. J. Chem.* **1959**, *37*, 803. (c) Grunwald, E.; Effio, A. *J. Am. Chem. Soc.* **1974**, *96*, 423.
(10) Abraham, M. H. *J. Chem. Soc., Perkin Trans. 2* **1973**, 1893.
(11) Kessler, H.; Fiegel, M. *Acc. Chem. Res.* **1982**, *15*, 2.
(12) Bateman, L. C.; Hughes, E. D.; Ingold, C. K. *J. Chem. Soc.* **1940**, 960.

0002-7863/87/1509-1891$01.50/0

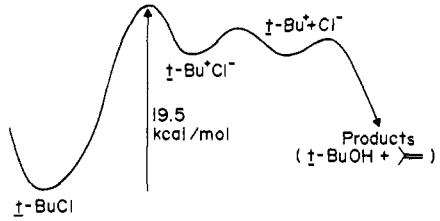

Figure 1. Schematic drawing of a possible reaction profile for the solvolysis of $(CH_3)_3CCl$ in water.

or there is a substantial barrier to recombination of the ions. Though the kinetics are unimolecular, the stereochemistry of solvolyses of tertiary alkyl halides in protic solvents also typically shows 20–35% net inversion of configuration.[3,14] Consequently, significant solvent capture appears to occur at the contact ion pair stage and free tertiary alkyl cations are probably not important reaction intermediates.[15]

Clearly, detailed knowledge of the energy profile for hydrolysis of *t*-BuCl could help elucidate some of these issues and provide information on whether all of the species in the ion pair region for eq 1 appear as distinct energy minima and on their relative energies and intervening barriers. In the present study, attention has been confined to the ion pair region. Computation of the energy profile for the first step in eq 1 would require characterization of the effects of hydration on gas-phase energy surfaces for both the ground state (*t*-BuCl → *t*-Bu$^{\bullet}$ + Cl$^{\bullet}$) and an excited state (*t*-BuCl → *t*-Bu$^+$ + Cl$^-$).[16] The requisite ab initio quantum mechanical calculations for the energy surfaces and potential function development are beyond the limits of our current computational resources.

In the following, the methodology for the computations is first summarized. The results for the free-energy profiles are then presented, followed by the structural findings on the variation in hydration as a function of interionic distance.

Computational Procedure

Two approaches have been taken to computing the free-energy profile for the *t*-BuCl ion pairs: Monte Carlo (MC) simulations in the context of statistical perturbation theory and integral equation methods using extended RISM theory. Closely related calculations have previously been used to study S_N2[17-20] and addition[21] reactions in solution and alkali halide ion pairs.[7,22] In each case, a one-dimensional reaction coordinate has been defined and the free-energy variation or "potential of mean force" (pmf) has been determined along that path. The Monte Carlo calculations are typically performed for a system consisting of the reacting solutes plus ca. 250 solvent molecules in a periodic cell. For both types of calculations, it is first necessary to establish the solvent-solvent and solute-solvent potential functions that describe the interactions between the components in the system. For the present case, the missing element was a potential function for the *t*-Bu$^+$···H_2O interactions. This was obtained from ab initio calculations as summarized in the next section. Details on the two types of statistical mechanical calculations are then provided.

Potential Functions. In the present calculations for the ion pair region in the hydrolysis of *t*-BuCl, it has been assumed that complete ionization has occurred, i.e., *t*-Bu$^+$ and Cl$^-$ have unit

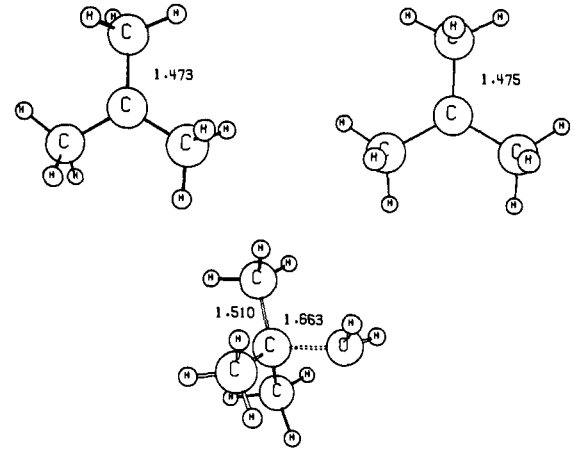

Figure 2. Computed geometries for $(CH_3)_3C^+$ in C_{3h} and C_{3v} symmetries and for $(CH_3)_3COH_2^+$ in C_s symmetry. Optimized with the 6-31G(d) basis set; the total energies in au are −156.44241, −156.44071, and −232.47816, respectively. Full **Z** matrices are available upon request.

charges at all separations. This seems reasonable in view of the variety of experimental measurements that indicate there is ca. 80% charge separation at the transition state for the S_N1 reaction of *t*-BuCl. These studies have been summarized by Abraham and include correlations between free energies of transfer for the S_N1 transition state and $(CH_3)_4N^+ + Cl^-$.[8] Thus, the charge separation for the contact ion pair should be essentially complete since it is farther along the reaction coordinate. This assumption simplifies the potential functions since the charge distributions and Lennard–Jones parameters for the ions can then be taken as invariant. Invariant parameters have been used in the earlier extended RISM calculations for alkali halide ion pairs[7] and for the computation of a pmf for Na^+Cl^- in TIPS2 water by Berkowitz et al.[22] The latter study employed molecular dynamics (MD) with importance sampling and is the only prior MC or MD determination of a pmf for an ion pair in water. Also, as in these earlier investigations, two-body potential functions have been used so polarization effects have not been explicitly included. This is obviously a significant approximation for any ionic solution, so the results must all be taken as quantitatively preliminary. However, this simplification should be less severe for larger, more charge delocalized ions as in the present case than for the smaller, charge localized alkali cations and F^-.

The potential functions that are then needed for the present calculations are for the *t*-Bu$^+$···H_2O, Cl$^-$···H_2O, and H_2O···H_2O interactions. The *t*-Bu$^+$···Cl$^-$ interaction is determined from the parameters developed independently for *t*-Bu$^+$ and Cl$^-$. As usual, the interactions are described in a Coulomb plus Lennard–Jones format (eq 2) where the sums are over interaction sites located

$$\Delta E_{ab} = \sum_{i}^{\text{on a}} \sum_{j}^{\text{on b}} (q_i q_j e^2/r_{ij} + A_{ij}/r_{ij}^{12} - C_{ij}/r_{ij}^{6}) \qquad (2)$$

on the ions or water molecules. For the Monte Carlo calculations, the TIP4P model has been used for water[23] along with previously reported parameters for Cl$^-$ that have been tested in MC simulations for Cl$^-$ in TIP4P water.[24] The parameters for *t*-Bu$^+$ were then determined from ab initio SCF calculations on *t*-Bu$^+$···H_2O complexes with the GAUSSIAN/82 program on a Gould 32/8750 computer.[25] The 6-31G(d) basis set was adopted and is of double-ζ quality with d-type polarization functions on all atoms except hydrogen.[26]

(13) Bunton, C. A.; Nayak, B. *J. Chem. Soc.* **1959**, 3854.
(14) Hughes, E. D.; Ingold, C. K.; Martin, R. J. L.; Meigh, D. F. *Nature (London)* **1950**, *166*, 679.
(15) Richard, J. P.; Jencks, W. P. *J. Am. Chem. Soc.* **1984**, *106*, 1373.
(16) Pross, A.; Shaik, S. S. *Acc. Chem. Res.* **1983**, *16*, 363.
(17) Chandrasekhar, J.; Smith, S. F.; Jorgensen, W. L. *J. Am. Chem. Soc.* **1985**, *107*, 154.
(18) Chandrasekhar, J.; Jorgensen, W. L. *J. Am. Chem. Soc.* **1985**, *107*, 2974.
(19) Jorgensen, W. L.; Buckner, J. K. *J. Phys. Chem.* **1986**, *90*, 4651.
(20) (a) Chiles, R. A.; Rossky, P. J. *J. Am. Chem. Soc.* **1984**, *106*, 6867. (b) Huston, S. E.; Rossky, P. J., to be published.
(21) Madura, J. D.; Jorgensen, W. L. *J. Am. Chem. Soc.* **1986**, *108*, 2517.
(22) Berkowitz, M.; Karim, O. A.; McCammon, J. A.; Rossky, P. J. *Chem. Phys. Lett.* **1984**, *105*, 577.
(23) (a) Jorgensen, W. L.; Chandrasekhar, J.; Madura, J. D.; Impey, R. W.; Klein, M. L. *J. Chem. Phys.* **1983**, *79*, 926. (b) Jorgensen, W. L.; Madura, J. D. *Mol. Phys.* **1985**, *56*, 1381. (c) Neumann, M. *J. Chem. Phys.* **1986**, *85*, 1567.
(24) Chandrasekhar, J.; Spellmeyer, D. C.; Jorgensen, W. L. *J. Am. Chem. Soc.* **1984**, *106*, 903.
(25) Binkley, J. S.; Whiteside, R. A.; Raghavachari, K.; Seeger, R.; DeFrees, D. J; Schlegel, H. B.; Frisch, M. J.; Pople, J. A.; Kahn, L. R. *Gaussian 82 Release H*; Carnegie-Mellon University: Pittsburgh, 1982. Converted to the Gould 32/8750 by Dr. J. D. Madura and J. F. Blake.

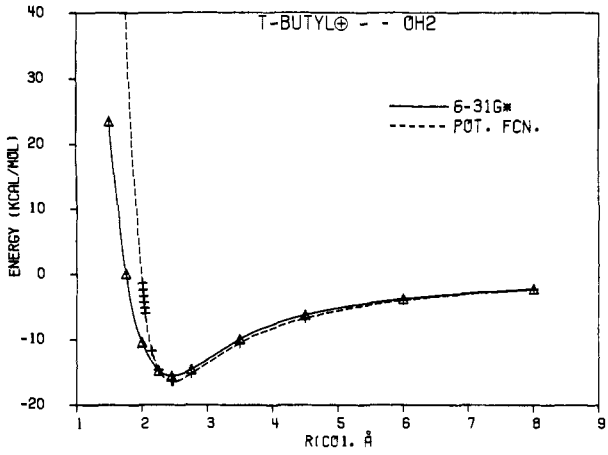

Figure 3. $(CH_3)_3C^+\cdots OH_2$ interaction energies as a function of C···O distance computed with the 6-31G(d) basis set and the potential functions. The oxygen is on the C_3 axis of the cation.

Full geometry optimizations were first carried out for *t*-Bu^+ in C_{3h} and C_{3v} symmetries and for protonated 2-methyl-2-propanol (*t*-$BuOH_2^+$) in C_s symmetry (Figure 2). The C_{3h} form of the ion was found to be 1.06 kcal/mol lower in energy than the C_{3v} alternative which is consistent with prior results with smaller basis sets.[27] The energy change for the reaction *t*-$Bu^+(C_{3h})$ + H_2O → *t*-$BuOH_2^+$ was then computed to be −15.7 kcal/mol. In order to compare this with Kebarle's experimental ΔH for the reaction,[28] vibrational frequencies for the reactants and products were obtained with the more economical 3-21G basis set which is well-suited for this purpose.[29] The zero-point energy change, $\Delta E_v°$, is +3.6 kcal/mol and the C_s form of *t*-$BuOH_2^+$ was shown to be a true energy minimum (no imaginary frequencies) at the 3-21G level. The thermal correction, $\Delta(\Delta E_v^{298})$, is +1.3 kcal/mol, and the changes in rotational and translational energy and $P\Delta V$ amount to $-4RT$. Combination yields a computed ΔH of −13.2 kcal/mol. The similarity to Kebarle's value of −11.2 kcal/mol was taken to be adequate enough to support use of the 6-31G(d) basis set in this context.

For the *t*-$Bu^+\cdots H_2O$ potential functions to be obtained, a series of 6-31G(d) calculations were subsequently carried out as a function of C–O distance with the oxygen on the C_3 axis of the C_{3v} ion (**1**). The monomer geometries were held fixed; the 6-

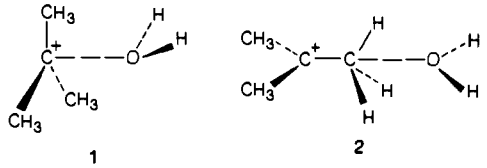

1 **2**

31G(d) optimized structure was used for the ion and the experimental geometry was adopted for water (r(OH) = 0.9572 Å, ∠HOH = 104.52°)[30] since this is also assumed in the TIP4P model. The flap angle between the C–O vector and the bisector of the HOH angle was optimized for each CO distance. The resultant interaction energy curve is given by the triangles in Figure 3. The minimum occurs at r(CO) = 2.45 Å with ΔE = −15.5 kcal/mol. Thus, the interaction energy is hardly changed from the fully optimized value for *t*-$BuOH_2^+$; however, the optimal r(CO) is shifted out by 0.8 Å when the carbon framework of *t*-Bu^+ is forced to be planar. The energy surface is clearly relatively flat with respect to coupled variations in r(CO) and the degree of pyramidalization. A second geometry was also considered in which the water molecule approaches a methyl group along a C–C bond (**2**). In this case, the optimal r(CO) is 3.01 Å with ΔE = −8.0 kcal/mol.

A simple model was adopted for *t*-Bu^+ with interaction sites centered on the four carbon atoms, i.e., the methyl groups are treated as united atoms as in the OPLS model for organic liquids and proteins.[31] The ion is planar with r(CC) = 1.475 Å. Since the TIP4P model is assumed for water, only one charge variable and the Lennard–Jones parameters for C and CH_3 can be optimized to fit the ab initio results. In fact, only the charge and the Lennard–Jones σ's were varied since the ϵ's were assigned from experience with other systems[31] and are not very important in the face of the dominant Coulombic interactions.

The final choice of parameters is summarized in Table I. The positive charge is distributed +0.40e on the central carbon and +0.20e on each methyl group. This may be compared with populations of +0.289e and +0.237e, respectively, from Mulliken analysis of the 6-31G(d) wave function for the C_{3v} ion. The resultant interaction energy curve for **1** is compared with the ab initio findings in Figure 3. The accord is good, though the repulsive wall rises too steeply which appears to be a general problem with 12-6 potentials in comparison to better ab initio calculations. The minimum from the potential function occurs at r(CO) = 2.47 Å with ΔE = −16.4 kcal/mol. The potential function and ab initio calculations also concur that the flap angle is essentially 180° for all C–O distances beyond 2.25 Å. In addition, the results for the second approach (**2**) compare well; the potential functions predict a minimum at r(CO) = 2.81 Å with ΔE = −8.14 kcal/mol.

The potential functions have also been used to calculate the interaction energy as a function of the CCO angle (Figure 4). For each value of θ, r(CO) and the flap angle were optimized. The distinct well found here centered at θ = 90° naturally results from the molecular structure of the cation. This contrasts the situation

Table I. Parameters for the Potential Functions

A. Monte Carlo Simulations[a]

site	q, e⁻	σ, Å	ϵ, kcal/mol
O	0.0	3.15358	0.15504
H	0.52	0.0	0.0
M[b]	−1.04	0.0	0.0
Cl	−1.00	4.417	0.118
C	0.40	2.250	0.050
CH_3	0.20	3.000	0.100

B. RISM Calculations[c]

site, j	$A_{Oj} \times 10^{-4}$	$C_{Oj} \times 10^{-2}$	$A_{Hj} \times 10^{-2}$
O	69.24	6.255	2.252
C	1.919	0.3868	0.0
CH_3	15.25	1.297	0.0
Cl	223.9	13.92	39.73

[a] In eq 2, $A_{ii} = 4\epsilon_i\sigma_i^{12}$, $C_{ii} = 4\epsilon_i\sigma_i^6$, $A_{ij} = (A_{ii}A_{jj})^{1/2}$, and $C_{ij} = (C_{ii}C_{jj})^{1/2}$. [b] M is a point on the bisector of the HOH angle, located 0.15 Å from oxygen toward the hydrogens. [c] A_{ij} in kcal·Å^{12}/mol, C_{Oj} in kcal·Å^6/mol.

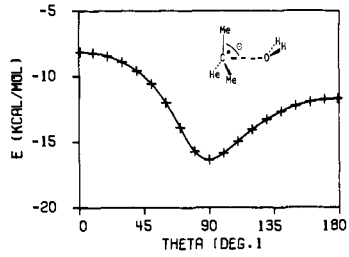

Figure 4. $(CH_3)_3C^+\cdots OH_2$ interaction energy as a function of the angle θ computed with the potential functions. C···O distance and the flap angle were optimized for each value of θ.

(26) Hariharan, P. C.; Pople, J. A. *Theor. Chim. Acta* **1973**, *28*, 203. Francl, M. M.; Pietro, W. J.; Hehre, W. J.; Binkley, J. S.; Gordon, M. S.; DeFrees, D. J.; Pople, J. A. *J. Chem. Phys.* **1983**, *77*, 3054.
(27) Radom, L.; Pople, J. A.; Schleyer, P. v. R. *J. Am. Chem. Soc.* **1972**, *94*, 5935.
(28) Hiraoka, K.; Kebarle, P. *J. Am. Chem. Soc.* **1977**, *99*, 360.
(29) Hehre, W. J.; Radom, L.; Schleyer, P. v. R.; Pople, J. A. *Ab Initio Molecular Orbital Theory*; Wiley: New York, NY, 1986.
(30) Benedict, W. S.; Gailar, N.; Plyler, E. K. *J. Chem. Phys.* **1956**, *24*, 1139.
(31) Jorgensen, W. L.; Tirado-Rives, J. *J. Am. Chem. Soc.*, in press, and references therein.

for spherical ions, such as the alkali cations, which have by symmetry perfectly flat corresponding profiles. The range of optimal geometries for t-Bu$^+$···H$_2$O interactions is clearly more restricted than that for the alkali ions.

Monte Carlo Simulations. The MC calculations were executed for the ion pair plus 250 TIP4P water molecules in the NPT ensemble at 25 °C and 1 atm. Standard procedures were employed as in earlier studies, including Metropolis and preferential sampling and periodic boundary conditions.[17-19,21] The periodic cell had dimensions that averaged ca. 17 × 17 × 26 Å. The pmf was determined as a function of the central carbon–chlorine distance (r_c) with the chloride ion maintained on the C_3 axis of the cation. The central carbon–chlorine vector was also kept parallel to the long axis of the periodic cell, though translations of the solutes were performed in tandem and the methyl groups were allowed to rotate about the C_3 axis.

The water–water and ion–water interactions were truncated with use of a procedure similar to Andersen's.[32] Specifically, the unscaled interaction energy, ΔE_{ab}, was multiplied by the scaling function given in eq 3. Thus, the interactions are feathered over

$$S(r_{OX}^2) = 1,\ r_{OX}^2 \le r_L^2$$
$$S(r_{OX}^2) = (r_U^2 - r_{OX}^2)/(r_U^2 - r_L^2),\ r_L^2 < r_{OX}^2 < r_U^2 \quad (3)$$
$$S(r_{OX}^2) = 0,\ r_{OX}^2 \ge r_U^2$$

a region between r_L and r_U. This quadratic switching function is computationally efficient in MC calculations where continuous derivatives are not essential. For the present computations, r_L and r_U were chosen to be 7.5 and 8.0 Å. Furthermore, the atoms of the ions were treated independently, so r_{OX} for the water–chloride interactions was r(OCl), and for the t-Bu$^+$, the four C–O distances were each considered; the interaction between a water molecule and the central carbon or a methyl group was evaluated, if r(CO) was less than r_U. For the water–water interactions, the entire interaction was included if r(OO) was less than r_U. This truncation scheme worked well with the perturbation calculations, though some alternatives such as simple, spherical truncation showed instability including occasional sudden jumps in the free energy changes.

The pmf was determined by using statistical perturbation theory[33] which has only recently been applied to a variety of other problems involving aqueous solutions including computation of the difference in free energies of hydration for ethane and methanol,[34] the effect of hydration on the structure of an S_N2 transition state,[19] and the relative free energies of binding of Cl$^-$ and Br$^-$ to an ionophore[35] and of benzamidine inhibitors to trypsin.[36] In all cases, the agreement with experimental data has been excellent and the precision of the method is impressive.

The approach follows from eq 4 which expresses the free-energy difference between systems 0 and 1 by an average of a function

$$\Delta G = G_1 - G_0 = -k_B T \ln \langle \exp[-(H_1 - H_0)/k_B T] \rangle_0 \quad (4)$$

of their enthalpy difference. The average is for sampling based on system 0, so system 1 is treated as a perturbation. Clearly, some care must be exercised to avoid overly large perturbations so the change may have to be broken into a series of small increments. In the present case, the theory has been used by sequentially perturbing along the reaction coordinate in steps of 0.125 or 0.25 Å. Double-wide sampling was used so 0.25 or 0.50 Å could be covered in one MC simulation.[34] For a perturbation of x Å, both ions were moved $x/2$ Å.

In all, 15 simulations were carried out to cover C–Cl distances between 2.5 and 8.0 Å. Each run consisted of an equilibration phase for at least 5 × 10^5 configurations, followed by averaging over an additional 1.5 × 10^6 or 2.0 × 10^6 configurations. New configurations were generated by randomly translating and rotating a randomly chosen water molecule or the ion pair. Ranges for the motions were selected to yield an acceptance ratio of ca. 0.4 for new configurations. The statistics for the ion pair were enhanced by attempting to move it every 60 configurations and by preferential sampling for the nearby water molecules with a standard algorithm.[24] Attempts to change the volume of the system were made every 1500 configurations.

$H_1 - H_0$ in eq 4 was evaluated as just the difference in the ion pair–water interaction energies and gives the difference in free energies of hydration, ΔG^{aq}.[34] Convergence of this quantity is generally facile, as illustrated below, and is helped by the preferential sampling. It is also reasonable that this difference should be relatively less sensitive to the cutoff distance for the interactions than the individual terms. Limited testing was performed on this point, as mentioned below, and supports the proposal, though more systematic study is warranted. The total free-energy change, ΔG^{tot}, is then given by the sum of ΔG^{aq} and the difference in interionic energies for the perturbation. The latter quantity was constant for a given perturbation since the chloride ion was kept on the C_3 axis of the cation.

The 15 MC simulations were executed on a Gould 32/8750. The BOSS program developed at Purdue was used and carefully optimized for these calculations; 1 × 10^5 configurations could be run in 96.5 min, so a total of 23 days of CPU time were required, or the equivalent of 3–4 months on a VAX 11/780. In contrast, the extended RISM calculations described next could be run in a few hours on a VAX.

Extended RISM Calculations. The potential of mean force was also obtained by solving the extended RISM integral equation[7,37,38] in much the same way as was done for an S_N2 reaction in earlier work.[20] Details of the integral equation formulation are not presented here, as they have been fully provided elsewhere.[37,38] The integral equation approach yields a set of approximate solute–solvent atom–atom radial correlation functions as the numerical solution to a set of coupled integral equations. The approximation made is embodied in the precise form of these equations. A number of earlier studies of a variety of aqueous systems have shown that the approach provides reliable qualitative predictions.[7,20,38,39]

For the technique to be applied in the present context, the five atomic-like sites in the t-Bu$^+$···Cl$^-$ ion pair were treated as a single molecular unit,[20] so that the relative geometry of approach of the chloride ion along the C_3 axis of t-Bu$^+$ can be fixed. The desired potential of mean force is then simply obtained from the excess chemical potential of this five-site solute in aqueous solution. The chemical potential was evaluated as a function of the "intramolecular" separation between the central carbon atom and the chloride ion, and the value at infinite separation was subtracted. The free energy computed directly in this way is that for the single ion pair at infinite dilution in an infinite amount of solvent; i.e., the calculation corresponds to constant solvent activity (equal to that of the bulk solvent). Thus, although the integral equations provide only approximate results, it is worth noting that, in contrast to simulation, no truncation of interaction potentials is used in the calculations.

The chemical potential was computed via the method reported by Singer and Chandler which directly utilizes the computed extended RISM solute–solvent correlation functions.[40] The technical implementation of the numerical solution of the integral equation and of the chemical potential calculation is identical with that described previously.[38]

One important result of the approximate nature of these calculations is the well-understood fact that the longest ranged part of the ion–ion potential of mean force in a polar solvent has the

(32) Andrea, T. A.; Swope, W. C.; Andersen, H. C. *J. Chem. Phys.* **1983**, *79*, 4576.
(33) Zwanzig, R. W. *J. Chem. Phys.* **1954**, *22*, 1420.
(34) Jorgensen, W. L.; Ravimohan, C. R. *J. Chem. Phys.* **1985**, *83*, 3050.
(35) Lybrand, T. P.; McCammon, J. A.; Wipff, G. *Proc. Natl. Acad. Sci. U.S.A.* **1986**, *83*, 833.
(36) Wong, C. F.; McCammon, J. A. *J. Am. Chem. Soc.* **1986**, *108*, 3830.
(37) Hirata, F.; Rossky, P. J.; Pettitt, B. M. *J. Chem. Phys.* **1983**, *78*, 4133 and references therein.
(38) Zichi, D. A.; Rossky, P. J. *J. Chem. Phys.* **1986**, *84*, 1712.
(39) (a) Rossky, P. J. *Pure Appl. Chem.* **1985**, *57*, 1043. (b) Pettit, B. M.; Rossky, P. J. *J. Chem. Phys.* **1982**, *77*, 509.
(40) Singer, S. J.; Chandler, D. *Mol. Phys.* **1985**, *55*, 621.

correct Coulombic functional behavior but with an obviously incorrect dielectric constant.[7,37] Nevertheless, this longest ranged Coulombic term can be analytically identified and separated from the remaining part of the calculation.[7,37] Hence, only the correction to a dielectric continuum theory is required of the theory. The dielectric result can be separately evaluated by using the solvent dielectric constant; both the experimental value and that for the TIP4P model are now available.[23c]

The interaction potentials used in the extended RISM calculation differ somewhat from those simulated. Solvent models including a minimum of interaction sites are computationally much simpler. Furthermore, for water models including an auxiliary site (not associated with a nuclear position) at a position very close to the oxygen (0.15 Å in TIP4P), we have found that the integral equation approach is less accurate, at least for the pure solvent. Therefore, the RISM calculations were carried out with use of the three-site SPC model of water (each site coinciding with an atom).[41] The model is characterized by an idealized molecular geometry (1 Å bond lengths and tetrahedral HOH angle), oxygen 6–12 parameters A_{OO} and C_{OO} (see Table IB), and charges $q_O = -2q_H = -0.82e$. These charges are used in combination with those in Table I.

If the full set of SPC water parameters is used directly to evaluate the ion–water potential functions according to the same combining rules as used with TIP4P (see Table I), an interaction results which is qualitatively, but not quantitatively, close to that used in the simulations. In order to make the comparisons here as meaningful as possible, we have treated the parameters of the *short ranged* ion–water potentials as adjustable in order to minimize the deviation between models. The minimization considers the energy difference between models for optimal solvent approach geometries over an ion–oxygen separation range of about 0.5 Å around the minimum. The resulting potential corresponds very closely to that used in the simulation, including agreement for the location and depth of the ion–solvent minima. The short-ranged (6–12) parameters derived from the minimization procedure, and used in the integral equation calculations, are listed in Table IB.

One further feature of these potentials should be noted. In most published water models, including SPC and TIP4P, no short-ranged interaction is associated with the solvent hydrogen position. A Coulomb singularity then exists when the solvent H coincides with either the solvent O of another molecule or, in the present case, the chloride ion. The removal of the singularity is not required in practice in simulation, since the simulations do not discover this region of configuration space. However, for the basically analytical integral equation theory such a singularity is not permitted. Therefore, an additional repulsive term of the form $A_{Hj}r^{-12}$ is included in the potential acting between the solvent hydrogen site and each oppositely charged interaction site j (i.e., water O and Cl^-). The values of A used are not of critical importance as long as the value is not either extremely small or larger than physically reasonable. The present work uses A_{HO} as in earlier work on pure water[39] and on conformational equilibria in water[38] and a value for A_{HCl}, as in earlier work[38] adjusted to the present Cl (see Table I). These values are notably small, and unobtrusive, compared to those characterizing other atomic pairs; the core terms remain less than the typical thermal energy RT until the hydrogen approaches a negatively charged site within about 2.0 Å or less, closer than the expected physical "contact" distance. At the potential minimum for $Cl^-\cdots H_2O$, the H–Cl core repulsion amounts to about 0.3 kcal/mol.

Results and Discussion

Potentials of Mean Force. The computed potentials of mean force are displayed in Figure 5, and the numerical data from the Monte Carlo simulations are in Table II. The figure includes the Monte Carlo and extended RISM results (using a dielectric constant of 78.36) as well as the "primitive model" prediction,

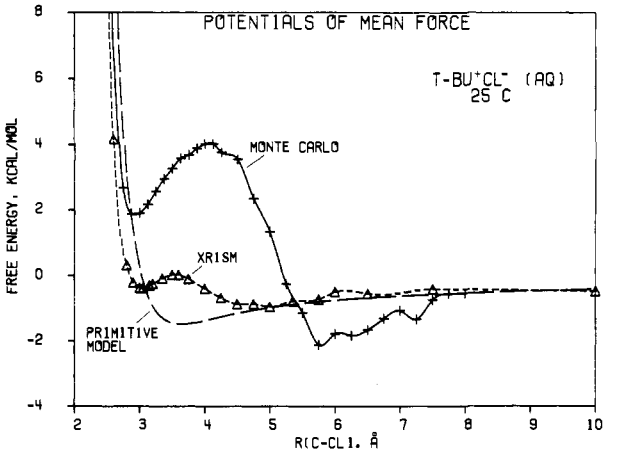

Figure 5. Calculated potentials of mean force for the dissociation of the $(CH_3)_3C^+Cl^-$ ion pair in water.

Table II. Results for the Potential of Mean Force from the Monte Carlo Simulations[a]

r(C–Cl)		ΔG^{aq}				
r_i	r_j	$i \rightarrow j$	$j \rightarrow i$	$\Delta\Delta G^{aq}(r_i)$	$\Delta E^{gas}(r_i)$	$\Delta G^{tot}(r_i)$
2.500	2.750		5.32	73.16	−62.27	10.89
2.750	2.875		2.39	67.84	−65.16	2.68
2.875	3.000	−2.38		65.45	−63.57	1.88
3.000	3.125		2.52	63.07	−61.17	1.90
3.125	3.250	−2.54		60.55	−58.38	2.17
3.250	3.375		2.57	58.01	−55.44	2.57
3.375	3.500	−2.57		55.44	−52.49	2.95
3.500	3.625		2.48	52.87	−49.60	3.27
3.625	3.750	−2.56		50.39	−46.82	3.58
3.750	3.875		2.34	47.83	−44.15	3.69
3.875	4.000	−2.27		45.49	−41.61	3.89
4.000	4.125		2.29	43.22	−39.20	4.03
4.125	4.250	−2.43		40.93	−36.91	4.03
4.250	4.500	−4.23		38.50	−34.74	3.77
4.500	4.750		4.83	34.27	−30.73	3.55
4.750	5.000	−4.29		29.44	−27.11	2.34
5.000	5.250		4.57	25.15	−23.83	1.33
5.250	5.500	−3.60		20.58	−20.85	−0.26
5.500	5.750		3.47	16.98	−18.13	−1.14
5.750	6.000	−1.96		13.51	−15.63	−2.12
6.000	6.250		2.17	11.55	−13.34	−1.78
6.250	6.500	−1.79		9.38	−11.22	−1.83
6.500	6.750		1.47	7.59	−9.26	−1.66
6.750	7.000	−1.45		6.12	−7.44	−1.31
7.000	7.250		1.84	4.67	−5.74	−1.07
7.250	7.500	−0.89		2.83	−4.16	−1.33
7.500	7.750		1.19	1.94	−2.69	−0.74
7.750	8.000	−1.29		0.75	−1.30	−0.55
8.000				(−0.54)	(0.0)	−0.54

[a] Distances in Å; energies in kcal/mol. ΔE^{gas}, the gas-phase energy difference, is relative to r(C–Cl) = 8.0 Å. The cumulative difference in free energy of hydration, $\Delta\Delta G^{aq}$, is anchored to the primitive model result at 8.0 Å.

which is obtained from the bare potential simply by dividing the interionic Coulombic interaction by the experimental dielectric constant.[42] The relative free energies obtained from the MC calculations have also been anchored to the primitive model result at 8.0 Å. Table II contains the incremental changes in the free energy of hydration, their total, the relative interaction energy for the ion pair in the absence of solvent, and the tabulated pmf. The statistical uncertainties in the Monte Carlo results are difficult to establish unequivocally. The fluctuations ($\pm 1\sigma$) in the incremental free energy changes averaged ±0.13 kcal/mol as obtained from separate averages over batches of 1×10^5 configurations. Since these uncertainties are cumulative, this implies a net uncertainty of ca. ±0.4 kcal/mol at the ends of the pmf if one starts

(41) Berendsen, H. J. C.; Postma, J. P. M.; von Gunsteren, W. F. In *Intermolecular Forces*; Pullman, B., Ed.; Reidel: Dordrecht, Holland, 1981; p 331.

(42) Vidulich, G. A.; Evans, D. F.; Kay, R. L. *J. Phys. Chem.* **1967**, *71*, 656.

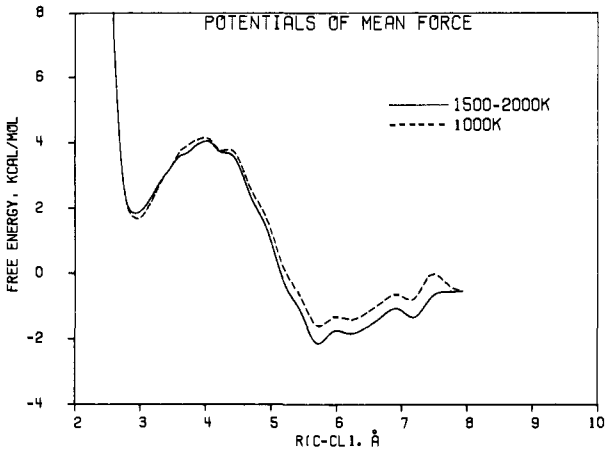

Figure 6. Comparison of the potentials of mean force obtained from the Monte Carlo simulations after 1×10^6 configurations of averaging and after $(1.5–2) \times 10^6$ configurations of averaging.

in the middle. The calculations do seem well-behaved, and, as mentioned above, the free-energy changes readily converge. This is illustrated in Figure 6 which compares the pmf obtained after averaging for 1×10^6 configurations in each run vs. the results after the calculations have been extended a further 50 to 100%. The quantitative differences are slight.

The Monte Carlo results show a well-defined minimum for a contact ion pair at a C–Cl distance of ca. 2.9 Å. The minimum for the solvent-separated form occurs at 5.75 Å; however, it is broad and the free energy appears to be just rising gradually beyond 5.75 Å. This means that "free ions" and the solvent-separated ion pair are probably not energetically distinct, separate entities. Extension of the simulations to r(C–Cl) = 10 Å would help clarify this point, though edge effects might start to interfere unless a larger periodic cell was used. In any event, the clear-cut finding of at least two distinct species in the ion-pair region is striking, and the importance of the solvent structure is obvious in comparison to the primitive model of a simple dielectric medium.

Quantitatively, the MC simulations predict a 2.1-kcal/mol barrier for conversion of the contact to the solvent-separated ion pair. The minimum for the latter is 4 kcal/mol lower in free energy and ca. 2 kcal/mol below the infinitely separated ions. Qualitatively, the results are reasonable and are not inconsistent with any of the experimental observations reviewed in the introduction. Abraham's conjecture[10] that the contact ion pair and free ions would be at about the same free energy may be compared with the computed difference of 2 kcal/mol. However, the approximations in the calculations do not guarantee that the relative energetic order for the contact and solvent-separated minima is correct. In fact, the extended RISM results for alkali halides in water indicate that the contact ion pair becomes relatively more favorable in progressing from Li^+ to K^+.[7] Though the preference for t-Bu^+Cl^- seems to run againt this trend, it can be rationalized since t-Bu^+ is significantly larger and more effective at shielding the anion than the alkali cations. Furthermore, the restricted angular preferences for the t-$Bu^+ \cdots H_2O$ interactions (Figure 4) may particularly disfavor the contact ion pair. As discussed in the following sections, the insertion of a water molecule into the favorable bonding position between the ions with θ near 90° (Figure 4) occurs between 5.00 and 5.75 Å and clearly helps stabilize the solvent-separated ion pair.

Some additional insight into the reliability of the calculations can be obtained by computing the heat of hydration for the ion pair. At separations between 6 and 8 Å, the sum of the solvent–solvent and solute–solvent energies was fairly constant at −2650 ± 10 kcal/mol. The total energy for 250 TIP4P water molecules can be estimated as −2515 ± 10 kcal/mol under the present conditions based on earlier work.[23b] Combination after a small PV correction[43] yields a heat of solution from the gas phase of −136 ± 14 kcal/mol for the ion pair at separations of 6–8 Å. From experimental data, single ion heats of hydration have been estimated for Cl^- and t-Bu^+ as −82 and −56.5 kcal/mol with uncertainties of 5–10 kcal/mol.[10,44] The total of −138.5 ± ca. 10 is similar to the computed value, though the latter can be expected to become more exothermic if the cutoff distance for the potential functions is increased[24] and as the interionic separation gets larger. For the present purposes, it is sufficient to note that the thermodynamics of hydration for the ion pair are not grossly in error.

The extended RISM results also find free energy minima for contact and solvent-separated ion pairs near 3.0 and 5.0 Å. However, the minima are now shallow and overall the pmf is much flatter than the Monte Carlo result. The same pattern was found previously in comparing the extended RISM and MD results for the pmf for Na^+Cl^- in water.[7,22] The source of the discrepancies is not known with certainty at this time. The application of integral equation theories to such complex systems is still in the formative stage and the approximate nature of the methodology should be kept in mind. For example, there are some structural inconsistencies in the extended RISM description of halide ion hydration that have been considered previously.[7] Several other possible origins for the quantitative discrepancies can also be mentioned. (1) The potential functions for the simulations and extended RISM calculations are not identical; however, the differences are quite small and it seems unlikely that they would produce the same qualitative pattern in two independent cases. (2) The experimental dielectric constant is used to rescale the Coulombic interactions in the extended RISM calculations, while the dielectic constant for TIP4P water has recently been computed to be 53.[23c] To test this effect the extended RISM results were rescaled with the lower dielectric constant; the modification to the curve in Figure 4 is qualitatively insignificant. The curve is just shifted down by an amount that decreases from 0.8 kcal/mol at 3.0 Å to 0.2 kcal/mol at 10 Å. (3) The effects of the finite system sizes and interaction cutoff procedures on the MC and MD results have not been established. In the present case, only a limited test was performed by increasing r_L and r_U by 0.5 Å to 8.0 and 8.5 Å for r_c = 5.25 ± 0.25 Å. Further increases are not possible without going to a larger periodic cell. This small change in cutoff distances did not produce statistically significant variations in the computed free energy changes. However, as mentioned above, sensitivity to the cutoff procedure was noted such that feathering the interactions produced greater stability in the perturbation calculations. In preliminary work, we also found that treatment of the solute atoms as independent particles seemed to be the most physically reasonable. With far larger system sizes and cutoff distances, it would probably matter little for the computation of the free-energy differences if, for example, a water molecule 20 Å away interacts with just a methyl group or with the methyl group and the remainder of the t-Bu^+ that might be a little more distant.

In closing this section, some other important technical points should be noted in view of the novelty of the perturbation calculations. It was found that the maximum free energy change that could be computed with acceptable precision in one step was not more than 5 kcal/mol. For example, when the perturbation from r_c = 3.75 to 3.50 Å was performed in one step, ΔG^{aq} = 5.54 ± 0.19 kcal/mol. Whereas, when the interval was divided in half and two perturbations were performed, the total ΔG^{aq} = 5.04 ± 0.16 kcal/mol. On the other hand, for r_c = 4.25 to 4.00 Å, the one- and two-step results were 4.59 ± 0.15 and 4.72 ± 0.16 kcal/mol. Another concern was that the simple act of moving the ions could provide artifactual contributions to ΔG^{aq}. This was tested in one simulation by translating the ion pair as a unit by ±0.125 along the long axis of the periodic cell rather than perturbing the ions in and out. After 5×10^5 configurations of averaging, the free-energy changes were both within 0.04 kcal/mol of 0.0. Finally, the compensation in the interionic and hydration

(43) Jorgensen, W. L.; Gao, J. *J. Phys. Chem.* **1986**, *90*, 2174.

(44) Bockris, J. O'M.; Reddy, A. K. N. *Modern Electrochemistry*; Plenum: New York, NY, 1970; Vol. 1, Chapter 2.

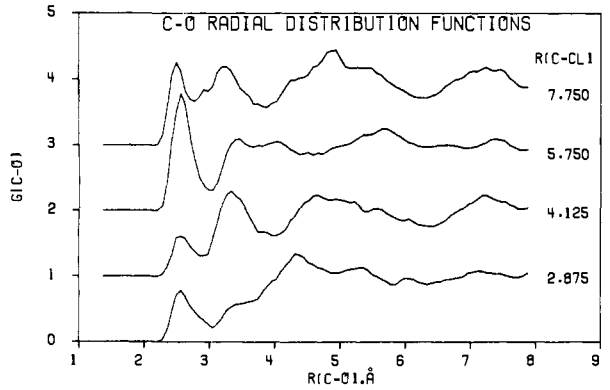

Figure 7. Central carbon–water oxygen radial distribution functions computed in the Monte Carlo simulations. Successive curves offset 1 unit on the y axis.

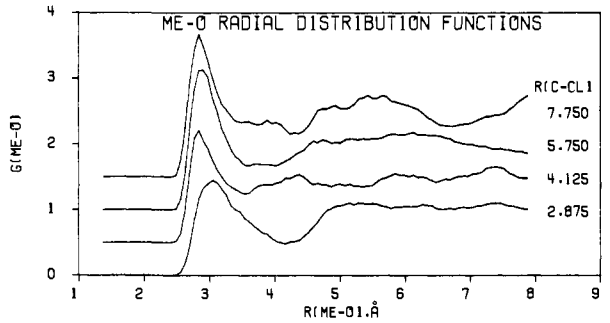

Figure 8. Methyl carbon–water oxygen radial distribution functions computed in the Monte Carlo simulations. Successive curves offset 0.5 unit on the y axis.

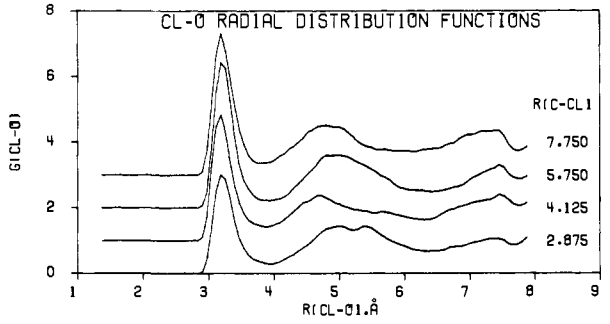

Figure 9. Chlorine–water oxygen radial distribution functions computed in the Monte Carlo simulations. Successive curves offset 1 unit on the y axis.

energies in Table II is remarkable. The ion–ion attraction decreases by 65 kcal/mol in going from 2.75 to 8.00 Å, while the free energy of hydration becomes more exoergic by a similar amount. The residual makes up the pmf in Figure 5. In the absence of water, the optimal ion–ion separation is 2.7 Å with an interaction energy of −107 kcal/mol.

Radial Distribution Functions. The changes in hydration that accompany separation of the ions were studied via radial distribution functions (rdfs), proximity analyses, and plots of configuration, as described here and in the next section. The rdf $g_{xy}(r)$ records the probability of occurrence of atoms with type y a distance r from atoms with type x, normalized for the bulk density of y atoms (N_y/V) and the volume element $4\pi r^2\,dr$. Six different atom–atom rdfs were obtained from both the Monte Carlo and extended RISM calculations. Some comparisons are made below, though the focus will be on the MC results.

The computed C–O, CH_3–O, and Cl–O rdfs from the MC simulations are shown in Figures 7–9 for four values of r_c, 2.875 Å (the contact ion pair), 4.125 Å (at the barrier top), 5.75 Å (the solvent-separated minimum), and 7.75 Å (the largest separation). For all three rdfs, the first peak is well-defined and can be integrated to obtain the number of nearest neighbors. The results are listed in Table III for many values of r_c; the integration limits were taken as 3.0, 3.5, and 3.85 Å for C–O, CH_3–O, and Cl–O to coincide roughly with the location of the first minima in the rdfs.

Table III. Computed Hydration Numbers from Integrating the First Peaks in the X–O Radial Distribution Functions[a]

	hydration numbers		
r_c, Å	C–O	CH_3–O	Cl–O
2.750	1.0	4.2	5.4
2.875	1.0	4.2	5.6
3.250	1.0	4.8	6.4
3.750	0.9	4.9	6.5
4.125	0.8	3.9	6.9
4.250	1.1	5.0	6.5
4.750	1.3	5.1	6.6
5.250	1.7	4.9	7.6
5.750	1.9	4.8	7.4
6.250	1.9	5.4	7.7
6.750	2.0	4.9	6.6
7.250	1.9	5.1	7.2
7.750	1.8	4.7	7.5

[a] Cutoff distances in Å: C (3.00), CH_3 (3.50), Cl (3.85).

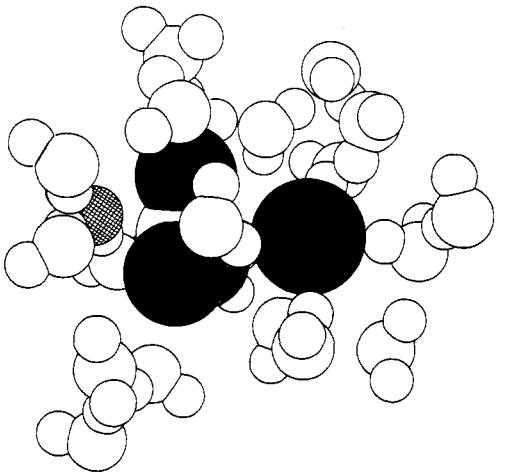

Figure 10. The $(CH_3)_3C^+Cl^-$ contact ion pair at a C–Cl separation of 3.0 Å. For Figures 10, 11, and 13, only water molecules with oxygens within 4.5 Å of any atom in the ion pair are shown. Taken from the last configuration of the Monte Carlo simulations which is as arbitrary as any other configuration. The hatched oxygens indicate water molecules solvating the carbenium carbon or between the ions. Methyl groups are shown as single atoms.

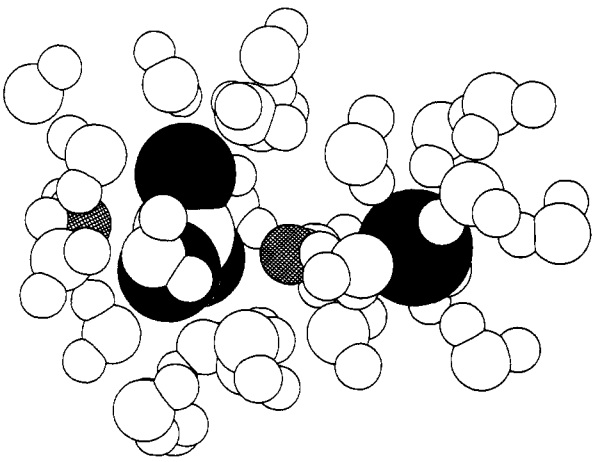

Figure 11. The $(CH_3)_3C^+Cl^-$ solvent-separated ion pair at a C–Cl distance of 5.75 Å. For additional details, see Figure 10.

The first peak in the C–O rdfs is centered at 2.5–2.6 Å which is consistent with the location of the minimum in Figure 3. Up

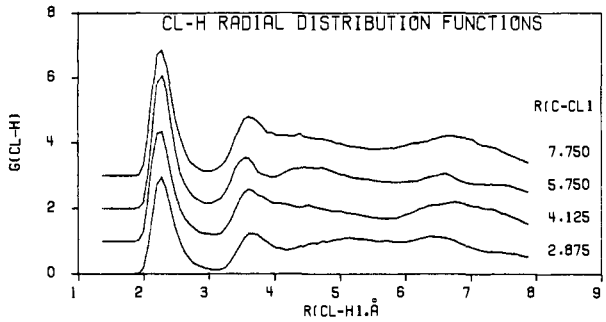

Figure 12. Chlorine–water hydrogen radial distribution functions computed in the Monte Carlo simulations. Successive curves offset 1 unit on the y axis.

to r_c = 4.25 Å its integral shows one water molecule that can be seen in plots of individual configurations, such as Figure 10, to be on the backside of the carbenium carbon. The first peak then doubles in area between 5.25 and 5.75 Å as a water molecule is inserted between the ions to form the solvent-separated ion pair. This is clearly illustrated by the configuration in Figure 11. Beyond the first peak in the C–O rdfs there is little striking structure except for r_c = 4.125 Å (Figure 7). A second peak centered at 3.3 Å is clear and is also found for r_c = 3.75 Å centered at 3.2 Å. The band contains 3–4 water molecules, one of which undoubtedly becomes the intervening water molecules in the solvent-separated ion pair. Thus, as the ions are separated, there is a buildup of water molecules off-axis between the two ions until there is enough room for one to be inserted on the axis. For r_c = 7.75 Å, the second band at 3.2 Å again becomes stronger, and the first peak is slightly reduced. At this separation, two water molecules are often between the ions and the one nearer the chlorine contributes to the second band.

The first peaks in the CH_3–O rdfs (Figure 8) are comparatively broad and contain 4–5 water molecules out to 3.5 Å for all values of r_c (Table III). The maxima occur near 3 Å which is consistent with the results from the optimizations for structure **2** described above. Overall, these rdfs are similar in appearance to the CH_3–O rdf for $(CH_3)_4N^+$ in water reported previously.[43] The charge of +0.25e used for the methyl groups of the ammonium ion is also similar to the charge of +0.20e on each methyl in $(CH_3)_3C^+$. Few additional insights are afforded by the C–H_O and CH_3–H_O rdfs, so they are not illustrated. However, they do confirm the expected dipole orientation for the water molecules since the locations of the first peaks in these rdfs show the water hydrogens are farther from the carbon atoms than the oxygens.

The first peak in the Cl–O rdfs (Figure 9) is centered at 3.2 Å and grows in height and area (Table III) as the ions separate. The location of the peak agrees with simulation results and diffraction data for chloride ion in dilute aqueous solution.[24,45] At r_c = 2.75 Å there are only 5.4 neighboring water molecules, though the number increases to 7–8 for r_c beyond 4.75 Å which is the same as for aqueous choride ion in the absence of the counterion.[24] Thus, at the contact ion-pair stage the t-Bu^+ shields the chloride ion from two potential first-shell water molecules. However, the shielding is no longer operative in the first hydration shell once the solvent-separated ion-pair region is entered.

Some orientational information can be extracted from the Cl–H_O rdfs in Figure 12. The strong first peaks clearly reflect the hydrogen bonding. The bands are centered at 2.2–2.3 Å which corresponds to an O–H bond length inside the first peaks for the Cl–O rdfs. Thus, the preference is for linear hydrogen bonding. This is confirmed by the similar integrals for the first peaks in the Cl–O and Cl–H rdfs and by the second bands in the Cl–H rdfs which are for the far hydrogens of the first-shell water molecules. The lack of bifurcated hydrogen bonds to the chloride ion is also apparent in Figures 10 and 11, except for the intervening water molecule in the solvent-separated ion pair.

Table IV. Computed Primary Hydration Numbers and Ion Pair–Water Interaction Energies (kcal/mol)[a]

	1° hydration no.			ion pair–water energy		
r_c, Å	C	CH_3	Cl	C	CH_3	Cl
2.75	1.0	2.8	4.7	−7.8	−2.7	−8.6
3.25	0.9	2.7	4.4	−10.4	−4.6	−8.6
3.75	0.5	3.0	4.2	−9.9	−6.6	−9.3
4.25	1.0	3.0	5.2	−11.4	−5.3	−9.7
4.75	0.8	2.8	5.6	−9.0	−7.0	−10.2
5.25	0.9	3.3	5.7	−15.4	−6.3	−10.2
5.75	1.7	2.9	6.5	−19.0	−5.8	−11.2
6.25	1.8	2.6	6.8	−17.3	−5.7	−11.2
6.75	1.7	2.6	6.6	−16.4	−5.8	−11.8
7.25	1.6	2.9	7.2	−12.6	−6.0	−10.6
7.75	1.1	2.7	7.5	−12.3	−6.6	−10.7

[a] Cutoff distances in Å: C (3.00), CH_3 (3.50), Cl (3.85).

The change in hydration beyond r_c = 5.75 Å is also interesting. Though no additional energy minima are evident in the pmf out to 8 Å, additional water molecules must start to enter the region between the ions. This is a gradual process in which the orientational possibilities for the hydrogen bonds can be very accommodating. An interesting illustration is provided by the configuration in Figure 13 at r_c = 7.25 Å. At least one water molecule is seen to be bridging between the water molecule on the frontside of the carbenium carbon and the chloride ion hydrogen bonding to both.

The trends in the extended RISM results for the rdfs and coordination numbers are qualitatively similar to the MC findings. For example, the number of main peaks and their positions for the C–O, CH_3–O, and Cl–O rdfs are in good accord. Furthermore, the hydration numbers for the central carbon and chlorine increase by ca. 1 and 2 as r_c extends from the contact to solvent-separated regions. However, the changes are much smoother. For example, the hydration numbers for the carbenium carbon at r_c = 3.00, 3.50, 4.25, and 5.75 Å are 0.99, 1.30, 1.53, and 1.55, respectively, while the simulation results have the hydration number constant at 1 till at least 4.25 Å, followed by a relatively rapid increase to 1.9 at r_c = 5.75 Å (Table III). Therefore, it seems that the extended RISM methodology is not feeling the coordinated effects of the molecular structures of the solvent molecules and solutes to a sufficient extent. In more technical terms, the excluded volume effects associated with the three-molecule correlation, t-Bu^+–H_2O–Cl^-, are not adequately represented, in accord with the approximations inherent in the theory. The smoother increases in the coordination numbers would be expected to correlate with a smoother pmf as is seen in Figure 5 and, in particular, lessen the barrier and the distinction between the contact and solvent-separated ion pairs.

Proximity Analyses. Further characterization of the coordination numbers and ion pair–water energetics can be obtained by proximiity analyses following the prescription of Mehrotra and Beveridge.[46] They defined a proximity criterion to assign first-shell solvent molecules to atoms of the solute. This requires a cutoff distance for each type of atom, so we have used the same cutoffs as for the first bands in the rdfs. Then, if a water molecule is nearer one atom than any other in the ion pair, it can be counted as in the primary hydration shell for the atom.

The computed primary coordination numbers obtained in this way from the MC simulations are given in Table IV. The table also contains the average interaction energies between the entire ion pair and the primary water molecules for each atom in the ion pair. The results were obtained from analysis of only 75 or 100 configurations that were saved at intervals of 2×10^4 configurations during each MC run. Thus, there are significant uncertainties of ca. ±0.3 for the coordination numbers and ±1–2

(45) Neilson, G. W.; Enderby, J. E. *Annu. Rep. Prog. Chem. Sect. C* **1979**, *76*, 185. Enderby, J. E.; Neilson, G. W. *Rep. Prog. Phys.* **1981**, *44*, 38. Newsome, J. R.; Neilson, G. W.; Enderby, J. E. *J. Phys. C.: Solid State Phys.* **1980**, *13*, L923. Cummings, S.; Enderby, J. E.; Neilson, G. W.; Howe, R. A.; Howells, W. S.; Soper, A. K. *Nature (London)* **1980**, *287*, 714.

(46) Mehrotra, P. K.; Beveridge, D. L. *J. Am. Chem. Soc.* **1980**, *102*, 4287.

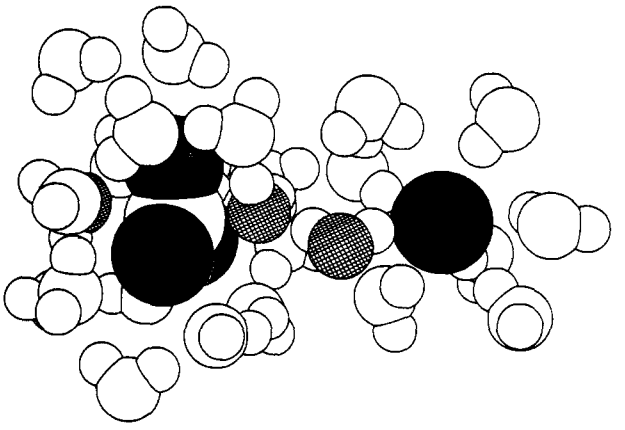

Figure 13. The $(CH_3)_3C^+Cl^-$ ion pair at a C–Cl separation of 7.25 Å. The rightmost hatched oxygen indicates a water molecule that is bridging between the chloride ion and the water molecule coordinated to the carbenium carbon. The latter's hydrogens are now oriented up to accommodate the hydrogen bond in contrast to Figure 11. 7–8 hydrogen bonds with the chloride ion are also clearly visible. For additional details, see Figure 10.

kcal/mol for the interaction energies.

Again, it is seen that 1 water molecule is associated with the carbenium carbon out to r_c = 5.25 Å, at which point a water molecule penetrates between the ions. The decrease in the primary hydration number at 7.75 Å may be partly statistical noise since the integral of the C–O rdf is still 1.8 (Table III). However, plots of configurations from the run at r_c = 7.75 Å do show an increase of disorder for the water between the ions. The interaction energies for the water molecules on the carbenium carbon show reasonable variations. Up to r_c = 5.25 Å, the water molecule on the backside of the t-Bu^+ has a net attractive interaction of ca. 10 kcal/mol with the ion pair. This value is less than for the minimum in Figure 3 because the orientation of this water molecule is clearly repulsive with respect to the chloride ion. Then between r_c = 5.25 and 6.75 Å the attraction is much greater because the water molecule between the ions interacts favorably with both. The attraction decreases to 12–13 kcal/mol beyond r_c = 7 Å because the distance to the chlorine is increasing.

The number of primary water molecules for each methyl group is constant at about 3. This is 1–2 less than the number of neighbors from integrating the CH_3–O rdf, so there are contributions from primary water molecules on the other solute atoms to the first band in the rdf. The average attractive interaction energy for the primary water molecules on the methyl groups is also relatively constant at 5–7 kcal/mol except for r_c below 3.75 Å. In this region, orientations of the water molecules that are particularly favorable for the cation are unfavorable for the nearby chloride ion, so the net attraction is diminished.

For the chloride ion, the primary hydration numbers are less than the integrals of the Cl–O rdfs (Table III) out to r_c = 6.25 Å. In this region, 1–2 water molecules with oxygens within 3.85 Å of the chlorine are closer to another solute atom. This is certainly the case for the intervening water molecule at r_c = 5.75 and 6.25 Å. However, beyond r_c = 6.25 Å the primary hydration numbers are identical with the integrals of the first peaks in the Cl–O rdfs. Thus, the separation between the ions is then great enough that the first shell of water molecules around the chlorine is distinct (Figure 13). Meanwhile, the average interaction energies for the primary water molecules on the chlorine with the ion pair become more favorable by roughly 2 kcal/mol between r_c = 2.75 and 7.75 Å. This is again associated with the fact that the water molecules on the backside of the chloride ion are oriented in an unfavorable way with respect to the cation. The energetic consequence is most severe at small interionic separations.

Conclusion

The present theoretical study has provided a view of the energetics and variations in hydration in the ion-pair region for the prototypical S_N1 reaction of t-BuCl in water. Support was found for the existence of a contact ion pair, while solvent-separated ion pairs and "free ions" do not appear to be energetically distinct species. The Monte Carlo results predict a significant barrier between the contact and solvent-separated ion-pair regions. The insertion of a water molecule between the ions occurs at separations of 5–5.5 Å and is preceded by a buildup of water molecules off the C–Cl axis. The computations involved state-of-the-art methodology in statistical mechanics; however, they still need to be considered preliminary, particularly in view of the simplicity of the potential functions that were used. The lack of polarization is especially a concern, though the nature of the perturbation calculations is such that some compensation of errors for the reference and perturbed systems is probable. The same is true for small errors in the balance between the interionic and ion–solvent interactions. The computationally efficient extended RISM approach was again found to reveal similar qualitative trends as the simuations. The origin of the quantitative differences requires further study; the present comparisons have suggested some areas for analysis.

Acknowledgment. Gratitude is expressed to the National Science Foundation (Purdue) and to the National Institute of General Medical Sciences (Texas) for support of this research. Computational assistance from Jiali Gao is also gratefully acknowledged.

Examination of Some Effects of NO_2 Rotation in Nitrobenzene

Peter Politzer,* Pat Lane, Keerthi Jayasuriya, and Linda N. Domelsmith

Contribution from the Department of Chemistry, University of New Orleans, New Orleans, Louisiana 70148. *Received September 15, 1986*

Abstract: A computational analysis has been made of some of the effects of rotating the NO_2 group of nitrobenzene by 90° from its equilibrium position in the plane of the aromatic ring. An ab initio SCF approach was used to compute the optimized structures and molecular electrostatic potentials of these two forms of nitrobenzene. A comparison of the calculated structures indicates that there is only a very small degree of conjugation between the nitro group and the aromatic ring in the equilibrium form of the molecule. Chemical consequences of NO_2 rotation are expected to include a decreased reactivity toward nucleophiles, but a slightly greater susceptibility to electrophilic attack.

I. Conjugation in Nitrobenzene

Nitrobenzene is commonly described in terms of resonance structures such as I–V. The NO_2 group is strongly electron withdrawing; this is usually attributed to induction and also the contributions of structures III–V, and accounts for the observed deactivation of the aromatic ring toward electrophilic attack.[1]

0002-7863/87/1509-1899$01.50/0